Bifurcations and chaos in a current-carrying ion sheath

Cite as: Physics of Fluids B: Plasma Physics 4, 3573 (1992); https://doi.org/10.1063/1.860365
Submitted: 28 February 1992 • Accepted: 17 July 1992 • Published Online: 04 June 1998

A. Komori, M. Kono, T. Norimine, et al.

Bifurcations and chaos in a current-carrying ion sheath

A. Komori, M. Kono,[a] T. Norimine, and Y. Kawai
Interdisciplinary Graduate School of Engineering Sciences, Kyushu University, Kasuga, Fukuoka 816, Japan

(Received 28 February 1992; accepted 17 July 1992)

Cascading bifurcations to chaos are investigated experimentally and theoretically in a current-carrying stable plasma. A dc plasma current is required to produce an electron-depleted thick sheath on a grid, which obeys the Child–Langmuir law of space-charge-limited current in a diode. Bifurcation cascade and chaotic behavior are exhibited when an external periodic oscillation is applied to the grid, and are in good agreement for the first time with a theory, which describes ion dynamics in the Child–Langmuir sheath and is represented by the differential equation with three independent variables. A fractal dimension predicted by the theory is verified by the experiment.

I. INTRODUCTION

It is of current interest to investigate nonlinear physical systems that exhibit chaotic behavior. Universal characteristics of chaos have been observed in experiments conducted on a variety of nonlinear media[1–4] as well as in numerical simulations.[5,6] Recently, several experiments have been reported on chaotic behavior in plasma systems.[7–12] Two routes to chaos, period doubling and intermittent chaos, are demonstrated in these experiments, and fine structures such as periodic windows are also observed. However, to our knowledge, the experimental observations of chaotic behavior in plasmas are not clearly understood and are still open to studies of their underlying physics, although they are explained to have the features given by the universal equations describing chaotic behavior.[13]

The present paper gives an experimental study of cascading bifurcations to chaos in a current-carrying plasma, and compares it with a theory which describes ion dynamics in a nonlinear potential well, formed as an ion sheath on the both sides of a grid by a dc plasma current.[14] A coherent instability appears when the thick ion sheath is formed on the grid and plasma parameters are properly selected.[15] In our previous paper, this instability was considered necessary for a set of cascading bifurcations and a chaotic state that are driven by the external oscillation.[11] In this work, however, cascading bifurcations to chaos are realized after stabilizing the plasma. Most properties of the oscillations, obtained experimentally, are consistent with those predicted theoretically.

The experimental apparatus is described in Sec. II. After describing the experimental results in Sec. III, a theory of bifurcations to chaos in our system is presented, compared with the experiment, and discussed in Sec. IV. The conclusion is given in Sec. V.

II. EXPERIMENTAL APPARATUS

The experiment is performed in a large, unmagnetized plasma device 70 cm in diameter and 120 cm in length, equipped with multidipole magnets for surface plasma confinement, as shown in Fig. 1.[11,15] An argon plasma produced by a dc discharge between filaments and the chamber wall is divided by a fine-meshed grid made of 0.05 mm diam stainless-steel wires spaced 0.5 mm apart. The discharge voltage V_d is in the 20–100 V range, and the chamber wall is electrically grounded. Typical parameters of the plasma designated T in Fig. 1 are $n_0=(0.9\text{–}7)\times10^8$ cm^{-3}, $T_e=0.3\text{–}0.7$ eV, and $T_i\simeq0.1$ eV, where n_0, T_e, and T_i are the plasma density, the electron temperature, and the ion temperature, respectively. Since T_e is roughly proportional to n_0 when V_d is low, V_d is adjusted to keep T_e independent of the change of n_0. The plasma density n_0 is controlled by changing the heater currents. At first, the density of the plasma D, n_{0D}, is chosen to be less than n_0 by about one order of magnitude, so that the plasma space potential ϕ_{0D} of the plasma D is higher than the plasma space potential ϕ_0 of the plasma T by a few volts. The symbol $\Delta\phi$ denotes the potential difference between ϕ_{0D} and ϕ_0 ($\Delta\phi=\phi_{0D}-\phi_0$). Plane Langmuir probes 6 mm in diameter are used to measure the plasma parameters and their fluctuations. The plasma space potentials are measured with emissive probes, and the ion temperature in the two plasmas is obtained with Faraday cups. The gas pressure p is usually kept at $\sim2\times10^{-4}$ Torr, and is sometimes varied in the range of $(1\text{–}4)\times10^{-4}$ Torr.

To drive a dc plasma current, a dc voltage V_0 is applied between the grid and a 12 cm diam target, that is, the grid and target are negatively and positively biased, respectively, as shown in Fig. 1. The target is located in the plasma T at a distance of 5 cm from the grid. The plasma current I_p flows mainly between the grid and target, since there are insulators on the reverse side of the target and both sides of the grid near the chamber wall. The potential drop on the grid, facing the plasma T, is considered to be almost equal to V_0 because ions, being more immobile than electrons, form a thick ion sheath so as to drive the ion current into the grid. On the other hand, the electron current flowing from the target can be driven by a small change of the potential drop on the target, which gives rise to the imbalance of electron and ion fluxes into the target. Here, we denote the sheath on the grid, facing the plasma

[a]Permanent address: Research Institute for Applied Mechanics, Kyushu University, Kasuga, Fukuoka 816, Japan.

 0899-8213/92/113573-06$04.00

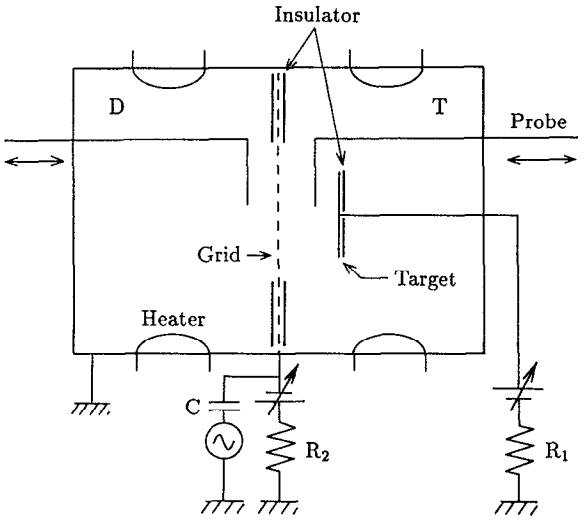

FIG. 1. Schematic of the experimental apparatus; $R_1=R_2=50\ \Omega$ and $C=3.3\ \mu$F.

T, by S_{GT}, and the sheath at the back of the grid by S_{GD}. The time-averaged value I_0 and fluctuating component I of I_p are observed from the voltage drop across the resistor R_1.

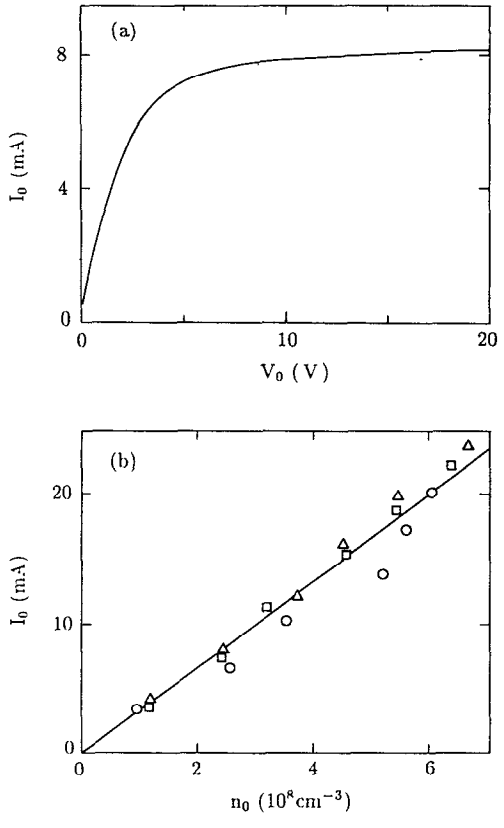

FIG. 2. Dependence of time-averaged value I_0 of the plasma current I_p on the dc voltage V_0 and on the plasma density n_0. (a) I_0-V_0 characteristic. (b) I_0 vs n_0. Circles, triangles, and squares are obtained at $V_0=30$, 60, and 90 V, respectively.

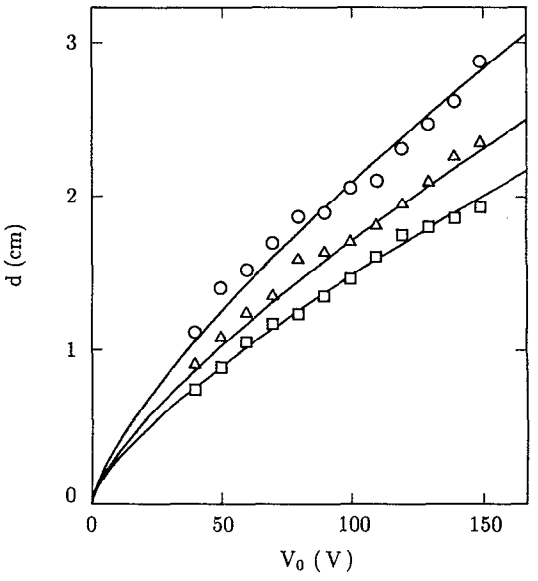

FIG. 3. Dependence of the thickness d of the sheath S_{GT} on the dc voltage V_0. Circles, triangles, and squares are obtained at $I_0=1$, 1.5, and 2 mA, respectively, and solid lines are proportional to $V_0^{3/4}$.

III. EXPERIMENTAL RESULTS

Figure 2(a) shows the dependence of the time-averaged current I_0 on the dc voltage V_0 between the grid and target. This I_0-V_0 curve is very similar to the current-voltage characteristic of the Langmuir probe, so that I_0 is expected to coincide with the Bohm current I_B. The Bohm current I_B is given approximately by[16]

$$I_B=Sn_0e(kT_e/m_i)^{1/2} \tag{1}$$

for $T_e \gg T_i$, where S is the area of the grid ($S\simeq 0.14\ \text{m}^2$) and m_i is the ion mass. The plasma density at the sheath edge is considered to be almost equal to n_0. The obtained plasma current I_0 agrees with I_B within a factor of 2, as expected, and the plasma parameter dependence of I_0 is well explained by Eq. (1). For example, I_0 is proportional to n_0, and does not depend on V_0, as shown in Fig. 2(b), where circles, triangles, and squares are obtained at $V_0=30$, 60, and 90 V, respectively. The plasma density n_0 is varied by controlling the heater currents. The sheath thickness d of the sheath S_{GT} is shown in Fig. 3, as a function of V_0. Circles, triangles, and squares are obtained at $I_0=1$, 1.5, and 2 mA, respectively, and solid lines represent the curves proportional to $V_0^{3/4}$. There is good agreement between the solid lines and measured d's. On the basis of these experimental results, the potential profile in the sheath S_{GT} is confirmed to be described by the Child–Langmuir law of space-charge-limited current in a plane diode:

$$I_0=(4\sqrt{2}\epsilon_0 S/9d^2)(e/m_i)^{1/2}V_0^{3/2}. \tag{2}$$

The sheath thickness d obtained experimentally is found to agree with the thickness given by Eq. (2) within a factor of

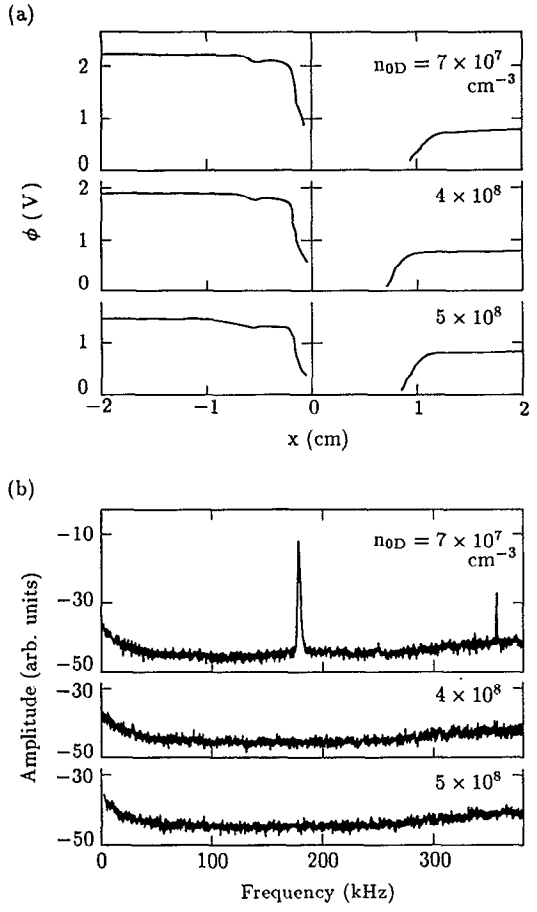

FIG. 4. Effect of the density of the plasma D, n_{0D}, on the potential ϕ around the grid and on the instability. (a) Axial profiles of ϕ for various n_{0D}'s. (b) n_{0D} dependence of frequency spectra of the perturbed plasma current I. The density n_{0D} is varied from 7×10^7 cm^{-3} to 5×10^8 cm^{-3}, while the density n_0 of the plasma T is kept at $\sim7\times10^8$ cm^{-3}.

3. This factor is associated with the reflection of ions from the plasma D to the plasma T by the potential difference $\Delta\phi$.[15]

At $V_0=0$ V, no fluctuation is observed in the plasma current I_p. A coherent instability appears when an extremely electron-depleted sheath is formed on the grid, that is, I_0 begins to saturate with an increase in V_0. An important point is that there is a threshold $\Delta\phi(=\phi_{0D}-\phi_0)$ to excite the instability. For example, when $\Delta\phi$ is as large as that shown in the top trace of Fig. 4(a), the instability is recognized in the frequency spectra of I, as shown in the top trace of Fig. 4(b) which is measured simultaneously with Fig. 4(a). Here, the origin of the x axis is located at the grid, and the x direction is pointed to the target. The potential ϕ near the grid, which is not shown in Fig. 4(a), drops nearer the grid and reaches the negative bias voltage at the grid. It is found that the frequency f_0 of the instability decreases with V_0, and that the amplitude of the instability is maximized in the relatively low V_0 range with a maximum percentage fluctuation level I/I_0 of $\sim5\%$.[15] The potential difference $\Delta\phi$ is considered to be necessary for reflecting ions which passed through the grid back to the plasma T, because the ion velocity given by the threshold $\Delta\phi$, $(2e\Delta\phi/m_i)^{1/2}$, agrees, roughly speaking, with the ion drift velocity v_0 at the sheath edge, which is obtained from Fig. 2(b) by using the relation of I_0 to n_0 and v_0. Many ions can pass through the grid, since the grid has a large ratio of the hole area to the whole area of the grid. If a metal plate is used instead of the meshed grid, no instability is observed, although a potential profile similar to that obtained with the meshed grid is measured between the grid and target.[15] The drift velocity v_0 is needed to satisfy the Bohm sheath criterion and to account for the loss of ions to the grid. The Bohm criterion says, as is well known, that ions must enter the ion sheath with a velocity v_0 faster than the ion-acoustic speed.[16]

The potential difference $\Delta\phi$, as shown in the top trace of Fig. 4(a), reflects ions that enter the sheath region from the plasma T, as mentioned above, so that a positive feedback mechanism is considered to be formed by these reflected ions which are bunched in a sense by a potential perturbation. The ion bunches are not neutralized by electrons in such an electron-depleted sheath. Thus, an ion resonance can be created in the ion-rich current-carrying sheath on the negatively charged grid. On the other hand, the exact relation linking the dc voltage V_{appl} of the power supply, the plasma current I_p, and the potential drop across the plasma V is given by $V_{\text{appl}}=V+(R_1+R_2)I_p$, so that the instability must be accompanied by a negative differential resistance $R=\partial V/\partial I_p$ of the plasma, which cancels out the resistance in the electric circuit. This negative rf resistance is associated with the ion inertia, and given in the electron-depleted sheath. On the basis of these results, the exciting mechanism of the instability has been identified as a negative rf resistance, coupled to an ion resonance.[15]

We now describe typical results of nonlinear behavior, obtained by applying an external periodic oscillation to the grid after stabilizing the plasma. By increasing the density n_{0D} of the plasma D, it is possible to stabilize the instability mentioned above. Figure 4(a) indicates that $\Delta\phi$ becomes small with an increase in n_{0D}. The density n_{0D} of the plasma D is varied from 7×10^7 cm^{-3} to 5×10^8 cm^{-3}, while the density n_0 of the plasma T is kept at $\sim7\times10^8$ cm^{-3}. Apparently, the decrease in $\Delta\phi$ leads to the stabilization of the instability, as shown in Fig. 4(b). The ion sheath S_{GT} is found to be affected little by the change of n_{0D}, so that there is the extremely electron-depleted ion sheath on the grid, as before, whose potential profile is described by the Child–Langmuir law. When an external periodic oscillation is applied to the grid under such a condition, a sinusoidal perturbation at the driving frequency can be induced in the plasma current I_p. Here, $f_1(=\omega_1/2\pi)$ and V_{ext} denote the frequency and amplitude of the external oscillation, respectively. Nonlinear behavior is observed by gradually increasing f_1 from 100 kHz and keeping V_{ext} at ~4.7 V. The first subharmonic appears at $f_1=139$ kHz, and a very clear period-doubling sequence is obtained, as shown in Figs. 5(a)–5(c). Further period doublings are hardly measured, possibly because the rapid convergence rate of the doubling sequence makes it very difficult to observe them. Increasing f_1 further produces

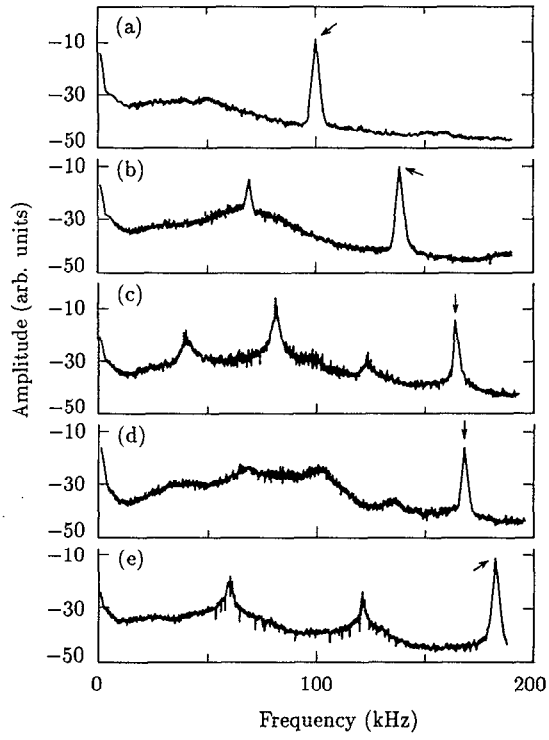

FIG. 5. Frequency spectra of the perturbed plasma current I; $n_0=1.2\times10^8$ cm^{-3}, $n_{0D}=8\times10^7$ cm^{-3}, $V_0=53$ V, and $V_{ext}=4.7$ V. (a)–(c) Frequency spectra of I for successive period doublings. (d) Chaotic spectrum corresponding to the nonperiodic oscillation. (e) Period tripling. The arrow indicates the driving frequency f_1. The spectrum amplitude scale is logarithmic.

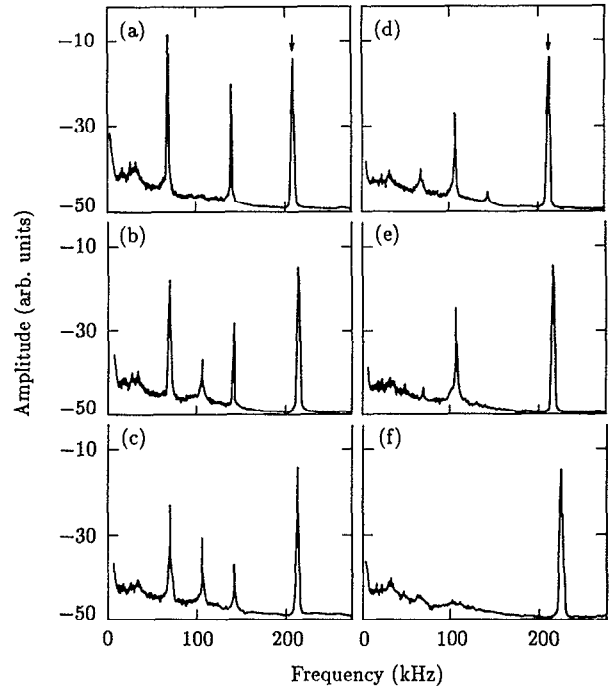

FIG. 6. Frequency spectra of the perturbed plasma current I; $n_0=9\times10^7$ cm^{-3}, $n_{0D}=1\times10^7$ cm^{-3}, $V_0=61$ V, and $V_{ext}=2.9$ V. The arrow indicates the driving frequency f_1, which increases in alphabetical order. The spectrum amplitude scale is logarithmic.

chaotic behavior. This state is characterized by broadband noise in the frequency spectrum, as shown in Fig. 5(d).[5,6] Further increases in f_1 cause period tripling [Fig. 5(e)]. Thus, it is clearly demonstrated that the bifurcation sequence leading to chaos in our system is the same as Feigenbaum's period-doubling route to chaos.

Nonlinear behavior of the oscillations is also realized by increasing n_0 with f_1 and V_{ext} fixed or increasing V_{ext} with f_1 and n_0 fixed. Although a set of cascading bifurcations to chaos is obtained when the neutral pressure p is changed in the range of $1\times10^{-4}\lesssim p\lesssim4\times10^{-4}$ Torr, whether p itself is relevant to the nonlinear behavior is not clear since n_0 is varied with the change of p. These observations are confirmed to be reproducible in our experiments. However, they are very sensitive to parameters such as n_0, V_{ext}, and so forth. For example, which appears first, period doubling or period tripling, depends on these parameters. Furthermore, a mixture of period-doubling and period-tripling bifurcations is sometimes observed. Figure 6 shows that period tripling occurs at first with an increase in f_1, but is followed by period doubling without passing through the chaotic regime. Thus, there are many scenarios of nonlinear behavior of the oscillations, depending on the parameters.

It is well known that a correlation dimension can give a noninteger dimension for a chaotic system, and yields a lower bound to the number N of degrees of freedom in the system.[17] Thus, to demonstrate that N is small in our system, the correlation dimension η is calculated using a time-dependent signal $I(t)$ measured experimentally. A trajectory in a k-dimensional space can be reconstructed by taking as coordinates $I(t)$, $I(t+\tau)$, $I(t+2\tau)$,..., $I[t+(k-1)\tau]$, where τ is an appropriate delay time.[18,19] In our experiments the time t is discretized, so that we obtain a series of k-dimensional vectors $\mathbf{r}_i$ representing the phase portrait of the dynamical system:

$$\mathbf{r}_i=\{I(t_i),\ I(t_i+\tau),\ I(t_i+2\tau),\ldots,\ I[t_i+(k-1)\tau]\},$$
$$i=1,\ 2,\ 3,\ldots,\ m. \tag{3}$$

The most used algorithm of calculating η was proposed by Grassberger and Procaccia.[17] With the series of vectors $\mathbf{r}_i$, one can evaluate the correlation sum $C(r)$ defined by

$$C(r)=\lim_{m\to\infty}\frac{1}{m^2}\sum_{i,j=1}^{m}H(r-|\mathbf{r}_i-\mathbf{r}_j|), \tag{4}$$

where H is the Heaviside function defined by $H(r)=1$ for positive r, 0 otherwise. For an intermediate region of r, $C(r)$ will scale like

$$C(r)\propto r^{\eta}. \tag{5}$$

In our experiments, the signals were digitized at 1–20 MHz with a transient recorder, and 128 kbytes of eight-bit data were recorded for each real-time signal. Choosing τ to be 1–4 μsec, η is obtained to be 1.54 ± 0.22 in the chaotic regime. This value of η suggests that the number of degrees of freedom is small in our system.

IV. COMPARISON WITH THEORY AND DISCUSSION

The ion sheath on both sides of the grid is regarded as a potential well in which the ions oscillate to give a primary motion responding to the external oscillation.[14] The structure and fluctuations of the ion sheath can be studied based on ion fluid:

$$\frac{\partial n}{\partial t}+\frac{\partial}{\partial x}nv=0, \tag{6}$$

$$\frac{\partial v}{\partial t}+n\frac{\partial}{\partial x}v=\frac{e}{m_i}E, \tag{7}$$

$$\frac{\partial E}{\partial x}=\frac{en}{\epsilon_0}. \tag{8}$$

For the stationary sheath, we have an implicit expression for E with respect to x as

$$x-x_0=\frac{eE_0}{m_i\omega_{pi}^2}\left[(1-A)\left(\frac{E}{E_0}-1\right)+\left(\frac{A}{3}\right)\left(\frac{E^3}{E_0^3}-1\right)\right],$$

$$A=(\omega_{pi}E_0\epsilon_0/I_0)^2/2, \tag{9}$$

where the suffix 0 means the value at the ion-sheath edge.

Now we consider the ion dynamics in the ion sheath given by Eq. (9). The ion dynamics is described by the following equations of motion:

$$\frac{dx}{dt}=v, \tag{10}$$

$$\frac{dv}{dt}=\frac{e}{m_i}(E_0-E). \tag{11}$$

In order to see the response to an oscillating external field, we consider, instead of Eq. (11),

$$\frac{dv}{dt}=\frac{e}{m_i}(E_0-E)-\nu v+E_{\text{ext}}\sin(\omega_1 t), \tag{12}$$

where the damping term is introduced because the bifurcations to chaos are observed experimentally in the dissipative system. From Eq. (9), we may approximately express E_0-E in terms of $(x-x_0)/(eE_0/m_i\omega_{pi}^2)\equiv x$ as

$$\frac{E_0-E}{E_0}\simeq-\frac{x}{1+A[x+(1-3A)x^2/3]}. \tag{13}$$

Combining Eqs. (10), (12), and (13) and replacing E_0 by $-|E_0|$ because of choosing E_0 negative, we finally have

$$\frac{d^2x}{dt^2}+\nu\frac{dx}{dt}+\frac{x}{1+A[x+(1-3A)x^2/3]}$$

$$+E_{\text{ext}}\sin(\Omega t)=0, \tag{14}$$

where $\omega_{pi}t$, ν/ω_{pi}, ω_1/ω_{pi}, and $E_{\text{ext}}/|E_0|$ are replaced by t, ν, Ω, and E_{ext}, respectively. The experimental conditions can be expressed in these normalized parameters. In Fig. 5, Ω is 0.382 (period two), 0.452 (period four), 0.471 (chaos), and 0.507 (period three) at $A\simeq0.192$, $\nu\simeq0.1$, and $E_{\text{ext}}\simeq2.29$; and Ω in Fig. 6 is 0.67 (period three) and 0.68 (period two) at $A\simeq0.224$, $\nu\simeq0.1$, and $E_{\text{ext}}\simeq1.18$.

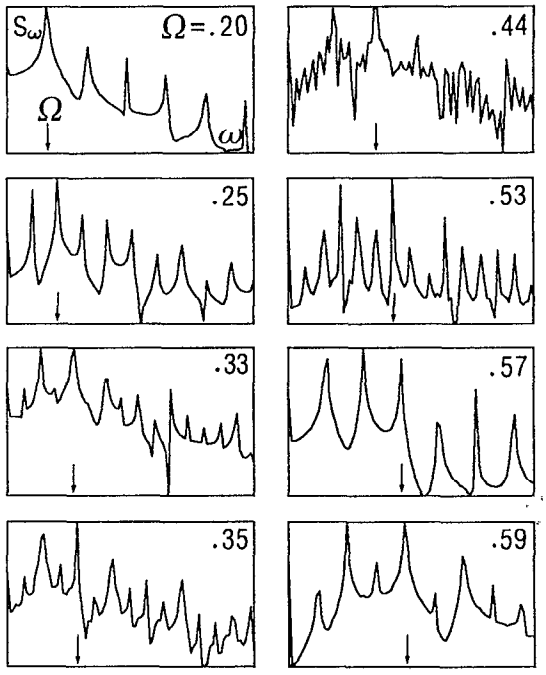

FIG. 7. Frequency spectra of x given by Eq. (14); $A=0.2$, $\nu=0.18$, and $E_{\text{ext}}=2.2$ for various Ω's. The spectrum amplitude scale is logarithmic and the horizontal axis represents the normalized angular frequency ω.

Equation (14) corresponds to a dynamical system with three independent variables, and reduces to a form of Duffing's equation by a simple transformation when A is small and the second term can be expanded with respect to A, indicating that Eq. (14) has many scenarios of nonlinear behavior of the oscillations. Figure 7 shows the Fourier spectra of $x(t)$ for various Ω's with $A=0.2$, $\nu=0.18$, and $E_{\text{ext}}=2.2$. Apparently, very clear period-doubling bifurcations to chaos are observed with an increase in Ω. Further increases in Ω cause period-tripling bifurcations. The same behavior of the oscillations is also observed by changing E_{ext} and keeping A, ν, and Ω constant.

The nonlinear behavior corresponding to that shown in Fig. 6 is also obtained numerically, when A and ν are chosen to be 0.225 and 0.1, respectively, with $E_{\text{ext}}=1.47$. As shown in Fig. 8, period tripling appears first, and then period doubling follows as Ω increases. This figure also shows that the state of period three alternates that of period two without passing through the chaotic regime. Like this, a rich variety of behavior can be realized by selecting the proper parameters.

The results revealed above agree surprisingly well with the experimental observations. The correlation dimension η, calculated using the time-dependent signal $x(t)$ given by Eq. (14), is obtained to be 1.54 ± 0.04, which also agrees with the experimental results $\eta=1.54\pm0.22$. Such a good agreement between experiment and theory indicates that the nonlinear behavior in our system is surely caused by the ion dynamics in the Child–Langmuir ion sheath.

V. CONCLUSIONS

A set of cascading bifurcations and a chaotic state in the presence of an external periodic oscillation are demon-

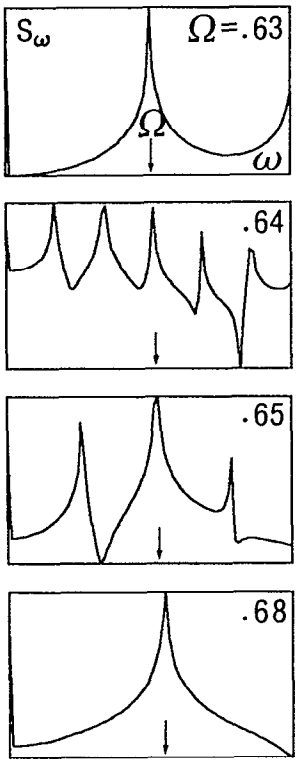

FIG. 8. Frequency spectra of x given by Eq. (14); $A=0.225$, $\nu=0.1$, and $E_{ext}=1.47$ for various Ω's. The spectrum amplitude scale is logarithmic and the horizontal axis represents the normalized angular frequency ω.

strated in a stable plasma by experimental results and a physical model. The most important point of this study is that the nonlinearity of a thick ion sheath on a grid causes a rich variety of behavior in our system. The thick ion sheath on the grid is formed by driving a dc plasma current, and described by the Child–Langmuir law of space-charge-limited current in a plane diode. A coherent instability associated with an ion transit in the sheath usually appears at the same time that the thick ion sheath is formed. This instability works to enhance nonlinear behavior of the system, but the cascading bifurcations to chaos can be realized even if the instability is not excited.

To explain the experimental results, the differential equation is used, which governs ion dynamics in an ion sheath potential well formed on the both sides of the grid. Bifurcations to chaos of the fluctuating current are obtained when an external oscillating term is added to the equation. Good agreement is found between theory and experiment, indicating that the nonlinear behavior in our system is attributed to the ion dynamics in an anharmonic potential well, that is, in the Child–Langmuir sheath. Finally, this work provides important information for the origin of nonlinear behavior which was observed experimentally in the various plasma systems.

ACKNOWLEDGMENTS

The authors wish to thank N. Ohno for his collaboration in the preliminary stage of the experiment, G. Miyashita for help with the data analysis, and M. Tanaka for many illuminating discussions. The authors would also like to acknowledge the continuing encouragement of N. Sato and H. Ikegami.

[1] A. Brandstäter, J. Swift, H. L. Swinney, A. Wolf, J. D. Farmer, E. Jen, and P. J. Crutchfield, Phys. Rev. Lett. **51**, 1442 (1983).
[2] H. Nakatsuka, S. Asaoka, H. Itoh, K. Ikeda, and M. Matsuoka, Phys. Rev. Lett. **50**, 109 (1983).
[3] S. D. Brorson, D. Dewey, and P. S. Linsay, Phys. Rev. A **28**, 1201 (1983).
[4] P. S. Linsay, Phys. Rev. Lett. **47**, 1349 (1981).
[5] M. J. Feigenbaum, J. Stat. Phys. **19**, 25 (1978).
[6] B. A. Huberman and J. P. Crutchfield, Phys. Rev. Lett. **43**, 1743 (1979).
[7] R. W. Boswell, Plasma Phys. **27**, 405 (1985).
[8] P. Y. Cheung and A. Y. Wong, Phys. Rev. Lett. **59**, 551 (1987).
[9] T. Braun, J. A. Lisboa, R. E. Francke, and J. A. C. Gallas, Phys. Rev. Lett. **59**, 613 (1987).
[10] P. Y. Cheung, S. Donovan, and A. Y. Wong, Phys. Rev. Lett. **61**, 1360 (1988).
[11] N. Ohno, M. Tanaka, A. Komori, and Y. Kawai, J. Phys. Soc. Jpn. **58**, 28 (1989).
[12] J. Qin, L. Wang, D. P. Yuan, P. Gao, and B. Z. Zhang, Phys. Rev. Lett. **63**, 163 (1989).
[13] P. Bergé, Y. Pomeau, and C. Vidal, *Order within Chaos* (Wiley, New York, 1986).
[14] M. Kono, H. Nakashima, and A. Komori, J. Phys. Soc. Jpn. **61**, 407 (1992).
[15] N. Ohno, A. Komori, M. Tanaka, and Y. Kawai, Phys. Fluids B **3**, 228 (1991).
[16] F. F. Chen, in *Plasma Diagnostic Techniques*, edited by R. H. Huddlestone and S. L. Leonard (Academic, New York, 1965), p. 150.
[17] P. Grassberger and I. Procaccia, Phys. Rev. Lett. **50**, 346 (1983).
[18] F. Takens, in *Dynamical Systems and Turbulence*, edited by D. A. Rand and L. S. Young (Springer-Verlag, Berlin, 1981), p. 366.
[19] N. H. Packard, J. P. Crutchfield, J. D. Farmer, and R. S. Shaw, Phys. Rev. Lett. **45**, 712 (1980).